

Quenched Degrees of Freedom in Symmetric Diblock Copolymer Thin Films

Wilfred H. Tang* and Thomas A. Witten

James Franck Institute, University of Chicago, Chicago, Illinois 60637

Received October 16, 1997; Revised Manuscript Received February 13, 1998

ABSTRACT: We studied the effect of monomer immobilization (quenching) on the orientation of the lamellae in symmetric diblock copolymer thin films with neutrally wetting surfaces. A small fraction of the monomers immediately next to the solid substrate is presumed to be quenched. Our calculations demonstrate that quenching favors the lamellae orienting perpendicular to the film. Quenching inhibits the order–disorder transition twice as much for the parallel orientation as for the perpendicular orientation.

1. Introduction

Bulk diblock copolymer melts have been studied extensively, both experimentally and theoretically.^{1,2} Recently, many studies have examined thin films of diblock copolymers. In this paper, we focus on symmetric diblock copolymers. In the bulk, symmetric diblock copolymers form lamellae upon microphase separation. In thin films, a variety of behavior has been observed. In some instances, the copolymers form lamellae parallel to the film interfaces.^{3–6} (see Figure 1a). Each of the two interfaces usually preferentially attracts one of the copolymer species. Having the lamellae parallel to the interfaces allows the maximum amount of favorable contact. However, in many experiments, other morphologies are observed.^{7–11} (See, for example, parts b and c of Figure 1.) Some of the results can be explained by confinement.^{12–16} Frustration resulting from the film thickness being incommensurate with the natural lamellar period can cause the morphology of Figure 1a to become energetically unfavorable. However, confinement does not appear to be sufficient to explain all of the experimental observations. In this paper, we studied the effect of monomer mobility on the morphology. There is reason to believe that, at least in some situations, the mobility of some monomers immediately adjacent to a solid substrate is greatly reduced.^{17–19} To make the calculation tractable, we assume that such monomers are completely immobilized (that is, *quenched*).

Our system is a thin polymer film of thickness h . Each polymer has $N/2$ monomers of some species A and $N/2$ monomers of species B, where A and B are assumed to be identical (i.e., same volume, segment length, etc.) except for their chemical potential. The $z = 0$ surface of the film is adjacent to a solid substrate, while the other surface, $z = h$, is free (in contact with air, for example). Since we are interested in the effect of quenching, not confinement, we assume that the film can adjust its thickness to eliminate any incompatibility between the film thickness and the natural lamellar period. We assume that the film thickness h is moderate–large compared to the chain root-mean-square end-to-end distance R_e but not so large that the bulk properties overpower the interfacial effects. A small fraction of monomers immediately adjacent to the solid substrate at $z = 0$ is assumed to be quenched. To

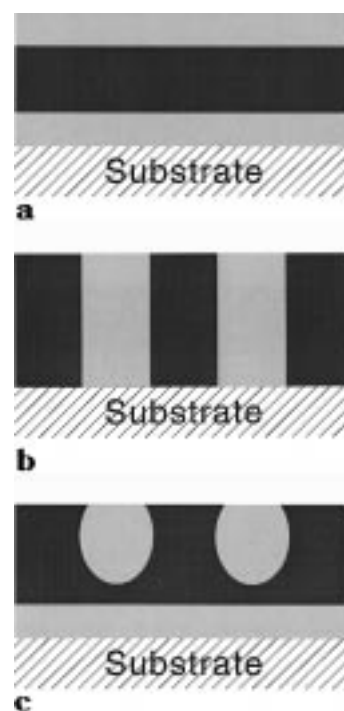


Figure 1. Some possible morphologies for thin films of symmetric diblock copolymers, as suggested by experiments.

simplify the calculation, we assume that the fraction of quenched monomers is sufficiently small that at most one monomer per chain is quenched. We also assume that it is equally likely for A and B monomers to be quenched. Finally, we assume that both the solid substrate and the free surface are neutral—that is, there is no preferential segregation of A or B monomers to the substrate or the free surface. This last assumption differs from the conditions in most experiments, though through careful design, it is possible to satisfy this last assumption.^{8,20,21} In future studies, we would like to eliminate this final assumption. Previous theories²² have treated the effect of surfaces on microphase separation, but they have not considered the effect of quenching. We show that monomer immobilization alone is sufficient to change the phase transition. It should be noted that the ability of quenching to alter the properties of materials in nonobvious ways has been demonstrated in a large variety of systems.^{23–26} For

example, the statistics of polymers in a quenched random environment differ from that of the corresponding annealed case,²⁴ and in spin glasses, quenched disorder has been studied in much detail over the years.²⁶

2. Weak Segregation Limit

Our formalism for the weak segregation limit is that of Marko and Witten^{27,28} and is similar in spirit to that of Leibler.²⁹ First, consider a reference (unquenched) system in which the A and B monomers are chemically identical—that is, each polymer chain consists of N identical monomers, the first half labeled A and the other half labeled B. The partition function for this system is

$$Z_{\text{ref}} = \int d\mathbf{R} e^{-S[\mathbf{R}]} \quad (1)$$

where $\int d\mathbf{R}$ is an integral over monomer positions of all chains and $S[\mathbf{R}]$ is the free energy arising from chain connectivity. The equilibrium average of an arbitrary quantity $X[\mathbf{R}]$ is given by

$$\langle X \rangle_{\text{ref}} = \frac{\int d\mathbf{R} e^{-S[\mathbf{R}]} X[\mathbf{R}]}{\int d\mathbf{R} e^{-S[\mathbf{R}]}} \quad (2)$$

Next, apply a perturbation free energy that arises from the immiscibility of A and B monomers

$$S = - \int d\mathbf{r} \mu(\mathbf{r}) \rho(\mathbf{r}) \quad (3)$$

where $\mathbf{r} = (x, y, z)$ denotes the three spatial coordinates, $\rho(\mathbf{r}) = \rho_A(\mathbf{r}) - \rho_B(\mathbf{r})$ is the order parameter for phase separation, and $\rho_A(\mathbf{r})$ and $\rho_B(\mathbf{r})$ are the local volume fractions of A and B monomers, respectively. (Note that $\rho_A(\mathbf{r}) + \rho_B(\mathbf{r}) = 1$.) The partition function for the perturbed system is

$$Z = \int d\mathbf{R} e^{-S[\mathbf{R}]} e^S \quad (4)$$

and the equilibrium average is given by

$$\langle X \rangle = \frac{\int d\mathbf{R} e^{-S[\mathbf{R}]} e^S X[\mathbf{R}]}{\int d\mathbf{R} e^{-S[\mathbf{R}]} e^S} \quad (5)$$

Since the weak segregation limit corresponds to small perturbations (small μ), we may express the order parameter as an expansion in the external potential μ

$$\langle \rho(\mathbf{r}_1) \rangle = \frac{\partial(\ln Z)}{\partial \mu(\mathbf{r}_1)} = G^{(1)}(\mathbf{r}_1) + \int d\mathbf{r}_2 G^{(2)}(\mathbf{r}_1, \mathbf{r}_2) \mu(\mathbf{r}_2) + \mathcal{O}(\mu^2) \quad (6)$$

where $G^{(1)}(\mathbf{r}_1)$ and $G^{(2)}(\mathbf{r}_1, \mathbf{r}_2)$ are defined as

$$G^{(1)}(\mathbf{r}_1) = \left. \frac{\partial(\ln Z)}{\partial \mu(\mathbf{r}_1)} \right|_{\mu=0} \quad (7)$$

and

$$G^{(2)}(\mathbf{r}_1, \mathbf{r}_2) = \left. \frac{\partial^2(\ln Z)}{\partial \mu(\mathbf{r}_1) \partial \mu(\mathbf{r}_2)} \right|_{\mu=0} \quad (8)$$

Using eq 4, we find that

$$G^{(1)}(\mathbf{r}_1) = \langle \rho(\mathbf{r}_1) \rangle_{\text{ref}} = 0 \quad (9)$$

and

$$G^{(2)}(\mathbf{r}_1, \mathbf{r}_2) = \langle \rho(\mathbf{r}_1) \rho(\mathbf{r}_2) \rangle_{\text{ref}} - \langle \rho(\mathbf{r}_1) \rangle_{\text{ref}} \langle \rho(\mathbf{r}_2) \rangle_{\text{ref}} = \langle \rho(\mathbf{r}_1) \rho(\mathbf{r}_2) \rangle_{\text{ref}} \quad (10)$$

Thus eq 6 can be rewritten (neglecting μ^2 and higher order terms) as

$$\langle \rho(\mathbf{r}_1) \rangle = \int d\mathbf{r}_2 G^{(2)}(\mathbf{r}_1, \mathbf{r}_2) \mu(\mathbf{r}_2) \quad (11)$$

In our copolymer melt, we use the Flory–Huggins form for the free energy perturbation³⁰

$$S_{\text{FH}} = \Lambda \int d\mathbf{r} \rho_A(\mathbf{r}) \rho_B(\mathbf{r}) = - \frac{\Lambda}{4} \int d\mathbf{r} \rho^2(\mathbf{r}) + \text{constant} \quad (12)$$

The demixing parameter³¹ Λ has units of inverse volume and is related to the Flory χ parameter³⁰ by $\Lambda V = \chi N$, where V is the chain volume and N is the number of monomers per chain. Using a mean-field approximation

$$\mu(\mathbf{r}) = - \left(\frac{\partial S_{\text{FH}}}{\partial \rho(\mathbf{r})} \right) = \frac{\Lambda}{2} \langle \rho(\mathbf{r}) \rangle \quad (13)$$

and eq 11 becomes an integral eigenvalue equation:

$$\langle \rho(\mathbf{r}_1) \rangle = \frac{\Lambda}{2} \int d\mathbf{r}_2 G^{(2)}(\mathbf{r}_1, \mathbf{r}_2) \langle \rho(\mathbf{r}_2) \rangle \quad (14)$$

For small values of Λ , the only solution to eq 14 is $\langle \rho(\mathbf{r}) \rangle = 0$ everywhere—that is, $\langle \rho_A(\mathbf{r}) \rangle = \langle \rho_B(\mathbf{r}) \rangle$ everywhere, and the copolymer melt is structureless. The smallest value of Λ which yields a nontrivial $\langle \rho(\mathbf{r}) \rangle$ marks the onset of microphase separation.

For a bulk copolymer melt, the results are well-known. $G^{(2)}(\mathbf{r}_1, \mathbf{r}_2) = 2 \langle \rho_A(\mathbf{r}_1) \rho_A(\mathbf{r}_2) \rangle_{\text{ref}} - 2 \langle \rho_A(\mathbf{r}_1) \rho_B(\mathbf{r}_2) \rangle_{\text{ref}}$ is readily calculated from random walk statistics. There can be no contribution to the $\langle \dots \rangle$'s unless \mathbf{r}_1 and \mathbf{r}_2 are on the same polymer. Thus the averages can be calculated by summing over all possible pairs of monomers along a single chain. It is convenient to label a monomer by the volume v displaced by the section of chain between that monomer and the A end of the chain. We label the monomer at \mathbf{r}_1 by v_1 and the monomer at \mathbf{r}_2 by v_2 . Thus

$$G^{(2)}(\mathbf{r}_1, \mathbf{r}_2) = \frac{2}{V} \int_0^{V/2} dv_1 \int_0^{V/2} dv_2 \times \left(\frac{a}{2\pi |v_1 - v_2|} \right)^{3/2} e^{-(a/2 |v_1 - v_2|) |\mathbf{r}_1 - \mathbf{r}_2|^2} - \frac{2}{V} \int_0^{V/2} dv_1 \int_{V/2}^V dv_2 \left(\frac{a}{2\pi |v_1 - v_2|} \right)^{3/2} e^{-(a/2 |v_1 - v_2|) |\mathbf{r}_1 - \mathbf{r}_2|^2} \quad (15)$$

where a is the “packing length”³² and V is the volume displaced by an entire chain. Since in this case

$G^{(2)}(\mathbf{r}_1, \mathbf{r}_2)$ depends on \mathbf{r}_1 and \mathbf{r}_2 through $\mathbf{r}_1 - \mathbf{r}_2$ only, the eigenvalue equation (eq 14) can be readily solved using Fourier transforms and the convolution theorem:

$$\langle \rho(\mathbf{k}) \rangle = \frac{\Lambda}{2} G^{(2)}(\mathbf{k}) \langle \rho(\mathbf{k}) \rangle \quad (16)$$

The onset of microphase separation occurs at $\Lambda^*V = 10.495$ and $k^* = 4.77/R_e$, where R_e is the root-mean-square end-to-end distance; $\langle \rho(\mathbf{r}) \rangle$ can be any sinusoidal function with a wavevector of magnitude k^* . A convenient basis set for $\langle \rho(\mathbf{r}) \rangle$ consists of functions of the form

$$\psi_i(\mathbf{r}) = \begin{Bmatrix} \cos(k_x x) & [k_x > 0] \\ 1 & [k_x = 0] \\ \sin(k_x x) & [k_x < 0] \end{Bmatrix} \times \begin{Bmatrix} \cos(k_y y) & [k_y > 0] \\ 1 & [k_y = 0] \\ \sin(k_y y) & [k_y < 0] \end{Bmatrix} \times \begin{Bmatrix} \cos(k_z z) & [k_z > 0] \\ 1 & [k_z = 0] \\ \sin(k_z z) & [k_z < 0] \end{Bmatrix} \quad (17)$$

where the factors in the three braces are multiplied together in all possible combinations such that $k_x^2 + k_y^2 + k_z^2 = k^{*2}$ is satisfied. (There are 26 total combinations; $1 \times 1 \times 1$ does not satisfy $k_x^2 + k_y^2 + k_z^2 = k^{*2}$.) Thus $\langle \rho(\mathbf{r}) \rangle = \sum_i a_i \psi_i(\mathbf{r})$, where the a_i are arbitrary constants. To obtain further information about the microphase separation, we must consider higher order terms not included in our formalism. Leibler²⁹ has calculated these higher order terms for all the possible morphologies consistent with $k_x^2 + k_y^2 + k_z^2 = k^{*2}$ and has found that the lamellar morphology is the most stable.

In the calculation described below, we calculate the effect of quenching before taking into account Leibler's higher order terms. This is reasonable if the perturbation to the microphase separation due to quenching is larger than the perturbation resulting from the higher order terms. We can also apply the perturbations in the opposite order. That is, we can first consider the higher order terms, which tell us that the most stable morphology is lamellar. We can then compare the effect of quenching on the different lamellar orientations. Such a calculation would be very similar to the one described below, and the final result does not change.

In a thin film, the boundaries at $z = 0$ and $z = h$ modify the bulk calculation slightly. We use Silberberg's chain-swapping procedure, which leads to reflective boundary conditions.^{33,34} Thus each of the two Gaussian terms in eq 15 should be replaced by

$$\exp\left[-\frac{a}{2|v_1 - v_2|} |\mathbf{r}_1 - \mathbf{r}_2|^2\right] + \exp\left[-\frac{a}{2|v_1 - v_2|} |\tilde{\mathbf{r}}_1 - \mathbf{r}_2|^2\right] + \exp\left[-\frac{a}{2|v_1 - v_2|} |\tilde{\mathbf{r}}_1 - \mathbf{r}_2|^2\right]$$

where $\tilde{\mathbf{r}}_1$ is the reflection of \mathbf{r}_1 in the $z = 0$ plane and $\tilde{\mathbf{r}}_1$ is the reflection of \mathbf{r}_1 in the $z = h$ plane. (Multiple reflections can be neglected because the film thickness h is large compared to the root-mean-square end-to-end distance R_e .) With this assumption, we find that, as in the bulk melt, $\Lambda^*V = 10.495$ and $k^* = 4.77/R_e$. However, the reflective boundary condition at $z = 0$ restricts the basis set functions $\psi_i(\mathbf{r})$ of eq 17 to functions that are even with respect to $z = 0$; that is, in the thin film,

$\langle \rho(\mathbf{r}) \rangle$ is a linear combination of

$$\psi_i(\mathbf{r}) = \begin{Bmatrix} \cos(k_x x) & [k_x > 0] \\ 1 & [k_x = 0] \\ \sin(k_x x) & [k_x < 0] \end{Bmatrix} \times \begin{Bmatrix} \cos(k_y y) & [k_y > 0] \\ 1 & [k_y = 0] \\ \sin(k_y y) & [k_y < 0] \end{Bmatrix} \times \begin{Bmatrix} \cos(k_z z) & [k_z > 0] \\ 1 & [k_z = 0] \end{Bmatrix} \quad (18)$$

where $k_x^2 + k_y^2 + k_z^2 = k^{*2}$. The reflective boundary condition at $z = h$ restricts $\psi_i(\mathbf{r})$ to functions that are even with respect to $z = h$; thus $k_z h = n\pi$, where n is a nonnegative integer.

The discussion above applies to unquenched systems. Applying the same formalism to quenched systems results in modifications to eqs 10 and 14

$$G_q^{(2)}(\mathbf{r}_1, \mathbf{r}_2) = \overline{\langle \rho(\mathbf{r}_1) \rho(\mathbf{r}_2) \rangle_{\text{ref},q}} - \frac{\overline{\langle \rho(\mathbf{r}_1) \rangle_{\text{ref},q} \langle \rho(\mathbf{r}_2) \rangle_{\text{ref},q}}}{\overline{\langle \rho(\mathbf{r}_1) \rangle_{\text{ref},q} \langle \rho(\mathbf{r}_2) \rangle_{\text{ref},q}}} \quad (19)$$

$$\overline{\langle \rho(\mathbf{r}_1) \rangle}_q = \frac{\Lambda}{2} \int d\mathbf{r}_2 \overline{G_q^{(2)}(\mathbf{r}_1, \mathbf{r}_2) \langle \rho(\mathbf{r}_2) \rangle}_q \quad (20)$$

where $\langle \dots \rangle_{\text{ref},q}$ and $\langle \dots \rangle_q$ denote equilibrium averages subject to the constraint q and the overbar denotes averaging over the constraints. In our system, the constraint is that a small fraction of the monomers immediately adjacent to the solid substrate at $z = 0$ cannot move.

The first term of $G_q^{(2)}(\mathbf{r}_1, \mathbf{r}_2)$ in eq 19 is equal to the first term of $G^{(2)}(\mathbf{r}_1, \mathbf{r}_2)$ in eq 10 since for any arbitrary quantity $X[\mathbf{R}]$, $\langle X \rangle_{\text{ref}} = \langle X \rangle_{\text{ref},q}$. However, while the second, residual term of $G^{(2)}(\mathbf{r}_1, \mathbf{r}_2)$ is zero, the residual term of $G_q^{(2)}(\mathbf{r}_1, \mathbf{r}_2)$ is nonzero. Using random walk statistics, we find that for a thin film with quenched monomers this residual term is

$$\overline{\langle \rho(\mathbf{r}_1) \rangle}_{\text{ref},q} \overline{\langle \rho(\mathbf{r}_2) \rangle}_{\text{ref},q} = 2 \overline{\langle \rho_A(\mathbf{r}_1) \rangle}_{\text{ref},q} \overline{\langle \rho_A(\mathbf{r}_2) \rangle}_{\text{ref},q} - \frac{2 \overline{\langle \rho_A(\mathbf{r}_1) \rangle}_{\text{ref},q} \overline{\langle \rho_B(\mathbf{r}_2) \rangle}_{\text{ref},q}}{\overline{\langle \rho_A(\mathbf{r}_1) \rangle}_{\text{ref},q} \overline{\langle \rho_B(\mathbf{r}_2) \rangle}_{\text{ref},q}} \quad (21)$$

where

$$\begin{aligned} & \overline{\langle \rho_A(\mathbf{r}_1) \rangle}_{\text{ref},q} \overline{\langle \rho_A(\mathbf{r}_2) \rangle}_{\text{ref},q} \\ &= 4\sigma \int dx' \int dy' \frac{1}{V} \int_0^V dv \int_0^{V/2} dv_1 \\ & \quad \left(\frac{a}{2\pi|v - v_1|} \right)^{3/2} e^{-(a/2|v - v_1|)[(x_1 - x')^2 + (y_1 - y')^2 + z_1^2]} \\ & \quad \int_0^{V/2} dv_2 \left(\frac{a}{2\pi|v - v_2|} \right)^{3/2} e^{-(a/2|v - v_2|)[(x_2 - x')^2 + (y_2 - y')^2 + z_2^2]} \\ &= \frac{4\sigma}{V} \int_0^V dv \int_0^{V/2} dv_1 \int_0^{V/2} dv_2 \\ & \quad \frac{a}{2\pi(|v - v_1| + |v - v_2|)} e^{-(a/2(|v - v_1| + |v - v_2|))[(x_1 - x_2)^2 + (y_1 - y_2)^2]} \\ & \quad \left(\frac{a}{2\pi|v - v_1|} \right)^{1/2} e^{-(a/2|v - v_1|)z_1^2} \left(\frac{a}{2\pi|v - v_2|} \right)^{1/2} e^{-(a/2|v - v_2|)z_2^2} \quad (22) \end{aligned}$$

and $\overline{\langle \rho_A(\mathbf{r}_1) \rangle}_{\text{ref},q} \overline{\langle \rho_B(\mathbf{r}_2) \rangle}_{\text{ref},q}$ is the same except that the integral of v_2 goes from $V/2$ to V instead of 0 to $V/2$. The quantity σ is the number of quenched monomers per

unit area at the $z = 0$ boundary. As noted above, we assume that the amount of quenching is sufficiently small that at most one monomer per chain is quenched. The integral $\int d\mathbf{x}' \int d\mathbf{y}'$ accounts for the fact that it is equally likely for any boundary location $(x', y', 0)$ to have a quenched monomer. The integral $1/V \int_0^V d\mathbf{v}$ accounts for the fact that it is equally likely for any monomer of each chain to be quenched.

Since the quenching density σ is small, $\langle \rho(\mathbf{r}_1) \rangle_{\text{ref,q}} \langle \rho(\mathbf{r}_2) \rangle_{\text{ref,q}} \ll \langle \rho(\mathbf{r}_1) \rho(\mathbf{r}_2) \rangle_{\text{ref,q}}$, and we can solve the eigenvalue equation 20 using degenerate perturbation theory.³⁵ We rewrite eq 20 as

$$\int d\mathbf{r}_2 \overline{[\langle \rho(\mathbf{r}_1) \rho(\mathbf{r}_2) \rangle_{\text{ref,q}} - \langle \rho(\mathbf{r}_1) \rangle_{\text{ref,q}} \langle \rho(\mathbf{r}_2) \rangle_{\text{ref,q}}]} \overline{\langle \rho(\mathbf{r}_2) \rangle_{\text{q}}} = \lambda \overline{\langle \rho(\mathbf{r}_1) \rangle_{\text{q}}} \quad (23)$$

where $\lambda = 2/\Lambda$. In the absence of quenching, the solution to eq 23 is $\lambda^{(0)} = 2/\Lambda^*$ and $\overline{\langle \rho(\mathbf{r}) \rangle_{\text{q}}}^{(0)} = \sum_i a_i \psi_i(\mathbf{r})$, where the $\psi_i(\mathbf{r})$ of eq 18 form a basis set for the unperturbed solutions and the a_i 's are arbitrary constants. In the presence of a small amount of quenching, we can perform an expansion in σ about $\lambda^{(0)}$ and $\overline{\langle \rho(\mathbf{r}) \rangle_{\text{q}}}^{(0)}$:

$$\lambda = \lambda^{(0)} + \sigma \lambda^{(1)} + \sigma^2 \lambda^{(2)} + \dots \quad (24)$$

$$\overline{\langle \rho(\mathbf{r}) \rangle_{\text{q}}} = \overline{\langle \rho(\mathbf{r}) \rangle_{\text{q}}}^{(0)} + \sigma \overline{\langle \rho(\mathbf{r}) \rangle_{\text{q}}}^{(1)} + \sigma^2 \overline{\langle \rho(\mathbf{r}) \rangle_{\text{q}}}^{(2)} + \dots \quad (25)$$

Applying degenerate perturbation theory and requiring that $\int d\mathbf{r} \psi_i(\mathbf{r}) \psi_j(\mathbf{r}) = 0$ for $i \neq j$, we can calculate $\sigma \lambda^{(1)}$ by solving

$$-\sum_i a_i \int d\mathbf{r}_1 \int d\mathbf{r}_2 \overline{\langle \rho(\mathbf{r}_1) \rangle_{\text{ref,q}} \langle \rho(\mathbf{r}_2) \rangle_{\text{ref,q}} \psi_j(\mathbf{r}_1) \psi_i(\mathbf{r}_2)} - \sigma \lambda^{(1)} a_j \int d\mathbf{r} \psi_j^2(\mathbf{r}) = 0 \quad (26)$$

From eqs 18, 21, and 22, we see that $\int d\mathbf{r}_1 \int d\mathbf{r}_2 \overline{\langle \rho(\mathbf{r}_1) \rangle_{\text{ref,q}} \langle \rho(\mathbf{r}_2) \rangle_{\text{ref,q}} \psi_j(\mathbf{r}_1) \psi_i(\mathbf{r}_2)} = 0$ for $i \neq j$.³⁶ Thus our original eigenfunctions ψ_i are already adequate to treat the perturbed system, and eq 26 reduces to

$$\sigma \lambda^{(1)} = - \frac{\int d\mathbf{r}_1 \int d\mathbf{r}_2 \overline{\langle \rho(\mathbf{r}_1) \rangle_{\text{ref,q}} \langle \rho(\mathbf{r}_2) \rangle_{\text{ref,q}} \psi_i(\mathbf{r}_1) \psi_i(\mathbf{r}_2)}}{\int d\mathbf{r} \psi_i^2(\mathbf{r})} \quad (27)$$

The integrals $\int d\mathbf{r}$, $\int d\mathbf{r}_1$, and $\int d\mathbf{r}_2$ range over the volume of the thin film. We assume that the extent of the film in the x and y directions is large enough that the x and y boundaries have a negligible effect. In the z direction, the integrals run from 0 to h . As noted above, h is assumed to be large compared to the polymer rms end-to-end distance R_e . Thus it is a good approximation to replace $\int_0^h dz_1$ and $\int_0^h dz_2$ in the numerator by $\int_0^\infty dz_1$ and $\int_0^\infty dz_2$.

For eigenfunctions with nonzero k_z

$$\psi_i(\mathbf{r}) = \begin{cases} \cos(k_x x) & [k_x > 0] \\ 1 & [k_x = 0] \\ \sin(k_x x) & [k_x < 0] \end{cases} \times \begin{cases} \cos(k_y y) & [k_y > 0] \\ 1 & [k_y = 0] \\ \sin(k_y y) & [k_y < 0] \end{cases} \times \begin{cases} \cos(k_z z) & [k_z > 0] \end{cases} \quad (28)$$

where $k_x^2 + k_y^2 + k_z^2 = k^{*2}$, we find that

$$\sigma \lambda^{(1)} = - \frac{4c\sigma V^2}{h} \quad (29)$$

and

$$\Lambda = \frac{2}{\lambda} \approx \frac{2}{\lambda^{(0)} + \sigma \lambda^{(1)}} \approx \Lambda^{(0)} \left(1 - \frac{\Lambda^{(0)}}{2} \sigma \lambda^{(1)} \right) = \Lambda^{(0)} \left(1 + \frac{2c\sigma V^2 \Lambda^{(0)}}{h} \right) \quad (30)$$

where $\Lambda^{(0)}$ corresponds to the microphase separation transition in the absence of quenching and c is a constant defined as³⁷

$$c \equiv \frac{1}{V^3} \int_0^V d\mathbf{v} \int_0^{V/2} d\mathbf{v}_1 \int_0^{V/2} d\mathbf{v}_2 e^{-\frac{|v-v_1|+|v-v_2|}{2a} k^{*2}} - \frac{1}{V^3} \int_0^V d\mathbf{v} \int_0^{V/2} d\mathbf{v}_1 \int_{V/2}^V d\mathbf{v}_2 e^{-\frac{|v-v_1|+|v-v_2|}{2a} k^{*2}} \approx 0.0204 \quad (31)$$

On the other hand, for eigenfunctions with $k_z = 0$

$$\psi_i(\mathbf{r}) = \begin{cases} \cos(k_x x) & [k_x > 0] \\ 1 & [k_x = 0] \\ \sin(k_x x) & [k_x < 0] \end{cases} \times \begin{cases} \cos(k_y y) & [k_y > 0] \\ 1 & [k_y = 0] \\ \sin(k_y y) & [k_y < 0] \end{cases} \times \begin{cases} 1 & [k_z = 0] \end{cases} \quad (32)$$

where $k_x^2 + k_y^2 + k_z^2 = k^{*2}$, we find that

$$\sigma \lambda^{(1)} = - \frac{2c\sigma V^2}{h} \quad (33)$$

and

$$\Lambda \approx \Lambda^{(0)} \left(1 + \frac{c\sigma V^2 \Lambda^{(0)}}{h} \right) \quad (34)$$

We are interested in the eigenfunctions with the smallest value of Λ . Thus, in the quenched system, the microphase separation transition occurs at Λ given by eq 34 and $\langle \rho(\mathbf{r}) \rangle = \sum_i a_i \psi_i(\mathbf{r})$, where the $\psi_i(\mathbf{r})$'s are given by eq 32 and the a_i 's are constants. Taking into account the higher order terms calculated by Leibler²⁹ further restricts $\langle \rho(\mathbf{r}) \rangle$ to lamellar morphologies. The only lamellar $\langle \rho(\mathbf{r}) \rangle$ that can be constructed using the $\psi_i(\mathbf{r})$ of eq 32 as basis functions are $\langle \rho(\mathbf{r}) \rangle = \cos(k_x x + k_y y + \theta)$ where $k_x^2 + k_y^2 = k^{*2}$ and θ is a phase constant—that is, the lamellae are perpendicular to the substrate, as in Figure 1b. (Notice that having lamellae parallel to the substrate—that is, $\langle \rho(\mathbf{r}) \rangle = \cos(k^* z)$ —would require $\psi_i(\mathbf{r})$ to be given by eq 28, corresponding to Λ given by eq 30. Since this is not the minimum value of Λ , the $\psi_i(\mathbf{r})$ given by eq 28 cannot be used.)

Thus quenching inhibits phase separation since quenching increases the value of the demixing parameter Λ at the order-disorder transition. Furthermore, quenching inhibits the formation of lamellae parallel to the substrate twice as much as lamellae perpendicular to the substrate. Consequently, quenching favors the lamellae orienting perpendicular to the substrate. From eq 34, we see that the amount of inhibition increases with increasing quenching density σ and decreases with

increasing film thickness h . Since quenching is an interfacial effect, increasing the volume of material relative to the interfacial area decreases the effect of quenching. We can also estimate the order of magnitude of the increase in Λ due to quenching. A large change in Λ would require large σ and small h . The largest monomer quenching density consistent with the assumptions in our calculation is $\sigma \approx a/V$, corresponding to about one quenched monomer per chain touching the substrate. Our formalism can handle higher quenching densities, but eq 22 would need to be modified to allow for more than one quenched monomer per chain. The smallest film thickness allowed by our calculation is $h \approx R_e \approx (V/a)^{1/2}$. Having h smaller than R_e would cause our calculation to break down in several places. Thus the largest possible perturbation consistent with our assumptions is

$$\frac{\Delta\Lambda}{\Lambda^{(0)}} = \frac{c\sigma V^2 \Lambda^{(0)}}{h} \approx c \frac{a^{3/2}}{V^{1/2}} \Lambda^{(0)} V \quad (35)$$

For a typical polymer, the chain volume $V \approx 10^5 \text{ \AA}^3$ and the packing length $a \approx 10 \text{ \AA}$, and we also know that $c \approx 0.02$ and $\Lambda^{(0)} V \approx 10$. Thus an upper bound on $\Delta\Lambda$ is $\Delta\Lambda/\Lambda^{(0)} \approx 0.02$, and the maximum $\Delta\Lambda$ that can actually be handled by our theory is probably much smaller. Nevertheless, this order of magnitude estimate demonstrates that the effect of quenching is not vanishingly small and cannot be completely ignored in interpreting experimental results.

3. Discussion

The calculation reported above describes the effect of immobilized monomers on block copolymer phase separation. We have shown that this immobilization tends to favor perpendicular lamellae. We have also shown how the immobilization constraint can be incorporated into the standard field theory used to treat polymer phase separation. On the other hand, our theory does not yet give an adequate account of why perpendicular lamellae are observed experimentally. Below we present an intuitive explanation of our results and discuss the various limitations in our theory, their experimental relevance, and the prospects for improving the theory.

We can gain some insight into why quenching favors perpendicular lamellae by considering the following strong segregation limit argument. In the strong segregation limit, symmetric diblock copolymers form lamellae consisting of regions of A monomers separated by sharp interfaces from regions of B monomers. In a thin film, the lamellae can orient either parallel or perpendicular to the substrate. In the absence of quenching, the free energies of these two orientations are equal, but this degeneracy is broken when there is quenching. Consider the effect of quenched monomers when the lamellae are parallel to the substrate, as in Figure 1a. Half of the quenched monomers are stuck in an unfavorable region. In order for a polymer chain containing an unfavorably quenched monomer to reach a favorable region, the disfavored chain segment must stretch a distance $L/4$, where L is the lamellar period, and this costs substantial free energy. Now consider the effect of quenched monomers when the lamellae are perpendicular to the substrate, as in Figure 1b. Again, half of the quenched monomers are stuck in an unfavorable region. In order for a polymer chain containing an unfavorably quenched monomer to reach a favorable

region, the disfavored chain segment must stretch a distance of *at most* $L/4$. Most chains containing an unfavorably quenched monomer need only stretch a shorter distance and thus incur a smaller free energy penalty. Therefore, quenching causes the lamellae to orient perpendicular to the substrate. While this argument is rigorously correct only in the strong segregation limit, the argument is suggestive of results in the intermediate segregation regime between the weak and strong segregation limits.

The most unrealistic assumption in our theory is that there is no preferential interaction of the A or B monomers with the surface. Such neutral surfaces are uncommon in practice. The reports of perpendicular lamellae that motivated this study^{7,9,10} were done on surfaces that were not at all neutral. Preferential interaction with the surface naturally favors a morphology in which the surface is covered with the preferred species. It thus opposes the tendency of the quenched chains to make perpendicular lamellae. The preferential surface interaction amounts to a perturbation in the free energy that is linear in the order parameter ρ . The perturbation due to quenching, on the other hand, is an effect quadratic in ρ : it does not break the A–B symmetry. Thus, for any significant phase separation amplitude, we expect the linear preferential adsorption term to dominate, unless its coefficient is zero (i.e., neutral surfaces).

In any case, even if the surfaces are nearly neutral, there are no lack of effects favoring perpendicular orientation, even without quenching. The effect of incommensurate thickness^{12–16} was already mentioned in the Introduction. In addition, nematic interactions between the monomers and the surface favor perpendicular lamellae.³⁸ Given all these restrictions, we do not expect quenching to play an important role in the weak segregation regime. In the strong segregation regime, the quenched chains carry a large free energy penalty and could play a much greater role. Our analysis of this regime is in progress.

Another restriction of our theory is the assumption of a small number of immobilized monomers. Under this assumption, the effect on the phase separation threshold Λ is of course small as well. Still, the calculation can give a glimpse of the effects of larger quenching density. If the quenched monomer density approaches one per chain touching the surface, the volume fraction of quenched chains near the surface becomes on the order of unity. Beyond this point our calculation becomes unreliable. As the number of immobilized monomers increases beyond this point, the surface chains become quenched at multiple sites, thus forming a series of grafted loops. One anticipates that these loops would inhibit microphase separation even more than the singly attached chains do, since the fluctuations that allow phase separation are more inhibited.

Our results are amenable to quantitative tests. Such tests would be of interest, as they would reveal how immobilization affects phase separation morphology. Naturally, one possible test is to induce block copolymer phase separation on a neutral surface containing a few grafted chains. Though we have only treated chains immobilized at an arbitrary monomer, our method is easily adapted to treat various cases—for example, end-grafted chains or chains grafted at the A–B junction point. One need only replace the average $1/V \int_0^V dv$ in

eq 22 by the appropriate superposition of v values. An experimental test could reveal the optimal way of influencing the morphology. It could also extend the understanding of the quenching effect beyond the narrow limits treated above. Such an experimental test, however, would face obstacles. Any residual nonneutrality of the surfaces would inhibit perpendicular orientation. In addition, nematic interactions with the surface would favor perpendicular orientation even in the absence of quenching, as noted above. A cleaner investigation could be performed using computer simulations. Here the neutral surface and the A-B symmetry of the chains could be realized exactly. Such simulations could help elucidate the interplay between the various factors, including preferential surface interactions, nematic interactions, film confinement, and quenching, that influence the phase separation morphology.

Acknowledgment. We thank Terry Morkved, Heinrich Jaeger, and Paul Mansky for helpful discussions. This work was supported in part by the MRSEC Program of the National Science Foundation under Award Number DMR-9400379. W.T. acknowledges support from the Department of Defense through an NDSEG Fellowship.

References and Notes

- Bates, F. S.; Fredrickson, G. H. *Annu. Rev. Phys. Chem.* **1990**, *41*, 525.
- Binder, K. *Adv. Polym. Sci.* **1994**, *112*, 181.
- Coulon, G.; Russell, T. P.; Deline, V. R.; Green, P. F. *Macromolecules* **1989**, *22*, 2581.
- Anastasiadis, S. H.; Russell, T. P.; Satija, S. K.; Majkrzak, C. F. *J. Chem. Phys.* **1990**, *92*, 5677.
- Coulon, G.; Ausserre, D.; Russell, T. P. *J. Phys. Fr.* **1990**, *51*, 777.
- Coulon, G.; Collin, B.; Ausserre, D.; Chatenay, D.; Russell, T. P. *J. Phys. Fr.* **1990**, *51*, 2801.
- Henkee, C. S.; Thomas, E. L.; Fetters, L. J. *J. Mater. Sci.* **1988**, *23*, 1685.
- Kellogg, G. J. et al. *Phys. Rev. Lett.* **1996**, *76*, 2503.
- Koneripalli, N.; et al. *Langmuir* **1996**, *12*, 6681.
- Morkved, T. L.; Jaeger, H. M. *Europhys. Lett.* **1997**, *40*, 643.
- Chaikin, P. M. Unpublished results.
- Kikuchi, M.; Binder, K. *J. Chem. Phys.* **1994**, *101*, 3367.
- Walton, D. G.; Kellogg, G. J.; Mayes, A. M.; Lambooy, P.; Russell, T. P. *Macromolecules* **1994**, *27*, 6225.
- Brown, G.; Chakrabarti, A. *J. Chem. Phys.* **1995**, *102*, 1440.
- Matsen, M. W. *J. Chem. Phys.* **1997**, *106*, 7781.
- Pickett, G. T.; Balazs, A. C. *Macromolecules* **1997**, *30*, 3097.
- Kremer, K. *J. Phys. Fr.* **1986**, *47*, 1269.
- Zheng, X.; et al. *Phys. Rev. Lett.* **1995**, *74*, 407.
- Frank, B.; Gast, A. P.; Russell, T. P.; Brown, H. R.; Hawker, C. *Macromolecules* **1996**, *29*, 6531.
- Mansky, P.; Liu, Y.; Huang, E.; Russell, T. P.; Hawker, C. *Science* **1997**, *275*, 1458.
- Mansky, P.; et al. *Phys. Rev. Lett.* **1997**, *79*, 237.
- Fredrickson, G. H. *Macromolecules* **1987**, *20*, 2535.
- Brereton, M. G.; Vilgis, T. A. *J. Phys. I Fr.* **1992**, *2*, 581.
- Cates, M. E.; Ball, R. C. *J. Phys. Fr.* **1988**, *49*, 2009.
- Chakraborty, A. K.; Shakhnovich, E. I. *J. Chem. Phys.* **1995**, *103*, 10751.
- Mezard, M.; Parisi, G.; Virasoro, M. A. *Spin Glass Theory and Beyond*; World Scientific: Singapore, 1987.
- Marko, J. F.; Witten, T. A. *Macromolecules* **1992**, *25*, 296.
- Dong, H.; Marko, J. F.; Witten, T. A. *Macromolecules* **1994**, *27*, 6428.
- Leibler, L. *Macromolecules* **1980**, *13*, 1602.
- de Gennes, P.-G. *Scaling Concepts in Polymer Physics*; Cornell University Press: Ithaca, NY, 1979.
- Roe, R. J.; Zin, W. C. *Macromolecules* **1980**, *13*, 1221.
- Fetters, L. J.; Lohse, D. J.; Richter, D.; Witten, T. A.; Zirkel, A. *Macromolecules* **1994**, *27*, 4639.
- Silberberg, A. *J. Colloid Interface Sci.* **1982**, *90*, 86.
- Our reflective boundary conditions are consistent with Fredrickson's boundary conditions in ref 22. His treatment allows for a demixing parameter Λ that is perturbed at the surface. We consider this perturbation to be negligible in our calculation.
- Courant, R.; Hilbert, D. *Methods of Mathematical Physics*; Interscience Publishers: New York, 1953; Vol. 1.
- We can simplify this calculation by making the following observations. Let us divide $\psi_i(\mathbf{r})$ into x , y , and z components: $\psi_i(\mathbf{r}) = \psi_{i_x}(x)\psi_{i_y}(y)\psi_{i_z}(z)$; similarly, $\psi_j(\mathbf{r}) = \psi_{j_x}(x)\psi_{j_y}(y)\psi_{j_z}(z)$. Equation 18 together with the relation $k_x^2 + k_y^2 + k_z^2 = k^{*2}$ show that if $i_x = j_x$ and $i_y = j_y$, then $i_z = j_z$ and thus $i = j$. Equivalently, $i \neq j$ implies that $i_x \neq j_x$ or $i_y \neq j_y$. Therefore, to show that $\int d\mathbf{r}_1 \int d\mathbf{r}_2 \langle \rho(\mathbf{r}_1) \rangle_{\text{ref,q}} \langle \rho(\mathbf{r}_2) \rangle_{\text{ref,q}} \psi_j(\mathbf{r}_1) \psi_i(\mathbf{r}_2) = 0$ for all $i \neq j$, it is sufficient to show that $\int d\mathbf{r}_1 \int d\mathbf{r}_2 \langle \rho(\mathbf{r}_1) \rangle_{\text{ref,q}} \langle \rho(\mathbf{r}_2) \rangle_{\text{ref,q}} \psi_j(\mathbf{r}_1) \psi_i(\mathbf{r}_2) = 0$ for all $i_x \neq j_x$ and for all $i_y \neq j_y$.
- While c is small, it is not unreasonably small since $1/c \approx 49$ is of the same order of magnitude as other constants in our problem, such as $\Lambda^{(0)}V \approx 10$ and $k^{*2}R_g^2 \approx 23$.
- Pickett, G. T.; Witten, T. A.; Nagel, S. R. *Macromolecules* **1993**, *26*, 3194.

MA971524V